Engineering Conferences International
ECI Digital Archives

The 14th International Conference on Fluidization – From Fundamentals to Products

Refereed Proceedings

2013

Gas-Fluidization and Flow Properties of Fine Lactose and Mineral Powders

Horng Yuan Saw
Massey University, New Zealand

Clive E. Davies
Massey University, New Zealand

Anthony H.J. Paterson
Massey University, New Zealand

Jim R. Jones
Massey University, New Zealand

GAS-FLUIDIZATION AND FLOW PROPERTIES OF FINE LACTOSE AND MINERAL POWDERS

Horng Yuan Saw[a,b], Clive E. Davies[a,b]*, Anthony H.J. Paterson[a] and Jim R. Jones[a]
[a]Massey University; School of Engineering and Advanced Technology, Palmerston North 4442, New Zealand
[b]Massey University; Riddet Institute, Palmerston North 4442, New Zealand
*T: +64-6-356-9099 ext. 7436; F: +64-6-350-5604; E: C.Davies@massey.ac.nz

ABSTRACT

Bed collapse tests were performed with fine lactose, sand and refractory dust. Standardized collapse time, t_c/H_{mf}, showed inverse proportionality to mean particle diameter, and direct proportionality to the cohesion of the bulk powder at zero applied stress.

INTRODUCTION

Lactose powders are important commodities in the food and pharmaceutical industries, where they are commonly used as ingredients in food formulations and as excipients and diluents in pharmaceutical dosage forms where the active agent is present as a dry particulate solid. Lactose powders can thus be subjected to a variety of processing operations involving particle-particle and particle-fluid interactions so their bulk characteristics and aeration properties are of immediate practical relevance.

Khoe *et al.* (1) advocated a multi-disciplinary approach involving particle characterization, powder rheology and fluidization, as being potentially rewarding in the understanding of powder behaviour. They found apparent correlation between $(\varepsilon_{mb}-\varepsilon_{mf})/\varepsilon_{mf}$ and adhesive force per particle calculated from shear cell measurements following the methods of Molerus (2,3); they generally cautioned that for complex powders, more than one parameter or mean diameter was required in the correlation of experimental results, but noted that their data correlated well with surface-volume mean diameter when size distributions were narrow. In a study of the role of inter-particle forces on fluidization of fine powders, Bruni *et al.* (4) discussed qualitative links between fluidization and shear cell measurements, suggesting that cohesion could explain fluidized-bed collapse results.

Powder cohesion, C, is a function of the compaction history undergone by a powder and can be determined from yield locus data measured with a shear cell; shear stress at failure is plotted against normal consolidation stress and C is the intercept of the yield locus on the shear stress axis. Cohesion data for milled lactose, for pre-consolidation stresses in the range 0.3–4.85 kPa, have been shown to correlate well with $[\sigma_{pre}/\sigma_{pre\text{-}min}]^n\ [\rho_B/(\rho_p\ d_{32})]$, where the variables in the correlation term were identified following consideration of the physical processes during shearing (5). A correlation proposed by Geldart and Wong (6) for their measurements on de-aeration rates of cohesive powders, albeit with a caveat on its use for predictive purposes, has "standardized collapse time", t_c/H_{mf}, inversely proportional to $[d_{32}]^{1.2}$ and $[\rho_p-\rho_g]^{1.4}$, and directly proportional to $\exp(1.074\ F_{45})$.

Powder cohesion obtained via shear cell measurements and t_c/H_{mf}, a fluidization parameter, share correlation variables and both are essentially inversely proportional to d_{32}; they could thus be expected to show some degree of correlation with each other. In a system without applied mechanical consolidation stresses or where overburden is low, as in a shallow fluidized bed, the powder cohesion parameter relevant to the settled state is C_0 and by inference, we surmise that C_0 will also show some degree of correlation with t_c/H_{mf}. In the work presented below, we examine data for lactose, and to cover a broader range of particle and powder characteristics have tested samples of sand and refractory dust as well. Powder tensile strength is also briefly discussed.

EXPERIMENTAL

Materials

The test materials were milled lactose coded LM and LP (5), spray-dried lactose coded LT, sand coded S, and refractory dust coded RD. Material physical properties are shown in Table 1; this table includes the estimates of cohesion and tensile strength at zero applied stress for each material. Particle density of lactose was obtained from the literature (7); the particle density of sand and refractory dust was measured with a specific gravity bottle and water. Particle size distribution was measured with the wet laser diffraction method (Mastersizer 2000, Malvern Instruments Ltd., UK); d^*_{32} has been determined by dividing the standard Mastersizer size data into bins equivalent to a BSS 410 sieve analysis (5). The solvent for lactose was isopropanol, and water was used for sand and refractory dust. The refractive indices for lactose, isopropanol, water, sand and refractory dust were 1.533, 1.378, 1.33, 1.48, and 1.76 respectively.

Fluidization apparatus

Figure 1 shows the fluidized bed setup used for bed collapse experiments and measurement of minimum fluidizing velocity, U_{mf}, and minimum bubbling velocity, $U_{mb,v}$; its key features have been reported elsewhere (8). The plenum chamber was packed with marbles for even gas distribution; it had a ¼" opening and a 1" opening at the bottom. A ¼" ball valve was installed close to the ¼" opening, and a 1" ball valve close to the other opening; the valves were used to control inlet gas flow and to vent gas from the chamber during bed collapse experiment. They

were connected physically with a chain and their opening and closing were synchronized; when one was fully open, the other was fully closed. A lever was used to control the degree of opening.

U_{mf}, was determined from the plot of bed pressure drop against superficial gas velocity, with increasing gas flow and $U_{mb,v}$ was the velocity at which bubbles were first observed visually in the powder bed. Bed height was read from the millimeter scale.

In each bed collapse test, the sample size was 500 g. Prior to measurement, the powder was fluidized vigorously for ~5 min. The superficial velocity was then set to ~2$U_{mb,v}$. Bed collapse began when the ¼" and 1" ball valves were respectively closed and opened to the maximum simultaneously and instantly. Change in bed height was recorded with a video camera (Model DMC-TZ20, LUMIX) at 30 frames per second and read against the millimeter scale. All experiments were done under ambient conditions. Bed collapse videos showed that the bed surface was relatively flat, and were analyzed frame by frame with computer software (QuickTime Player version 7.6.9); bed height was plotted against time. The time needed for linear bed collapse, the hindered settling zone, was determined graphically, and t_c/H_{mf} calculated.

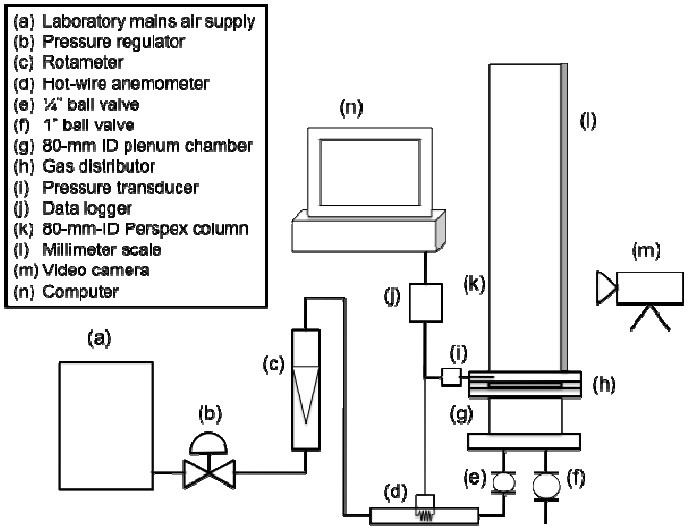

Figure 1 Schematic diagram of fluidized bed setup (not to scale)

Shear cell

An annular shear cell (Brookfield Engineering Laboratories Inc., USA) was used to measure powder cohesion, C, at pre-consolidation stresses, σ_{pre}, in the range 0.31–4.85 kPa (5). C was estimated from plots of shear stress at failure against normal stress; for example, see Figure 2 for model powder LP2 for the case of σ_{pre}=0.31 kPa. We have estimated C_0 by plotting C against σ_{pre} and extrapolating

to σ_{pre}=0; see Figure 3. Note that by inspection of the cohesion data for all the powders, we noticed that C generally increases monotonically up to σ_{pre}=1.2 kPa and we have used only data in the range [σ_{pre}=0] to [σ_{pre}=1.2] in the extrapolation to C_0. Tensile strength at σ_{pre}=0, T_0, was obtained by the same method.

Table 1 Physical properties and transitional superficial velocities of test powders.

Powder	ρ_p [kg m^{-3}]	d_{10} [µm]	d_{50} [µm]	d_{90} [µm]	d^*_{32} [µm]	Span [-]	F_{45} [-]	C_0 [kPa]	T_0 [kPa]	U_{mf} [m s^{-1}]	$U_{mb,v}$ [m s^{-1}]
Milled lactose											
LM2	~1540	27	113	191	73	1.45	0.121	0.0438	0.0773	0.00478	0.00591
LP2	~1540	36	139	232	84	1.41	0.110	0.0449	0.0766	0.00620	0.00734
LM3	~1540	82	143	219	111	0.96	0.047	0.0311	0.0532	0.00570	0.00733
LM6	~1540	142	242	387	164	1.01	0.045	0.0343	0.0577	0.01470	0.01630
LP3	~1540	178	263	373	223	0.74	0.018	0.0104	0.0176	0.02320	0.02320
Spray-dried lactose											
LT1	~1540	16	47	87	36	1.50	0.415	0.0456	0.0910	0.00204	0.00330
LT2	~1540	76	114	159	102	0.73	0.025	0.0168	0.0449	0.00645	0.01011
Sand											
S3	~2470	19	37	60	29	1.11	0.615	0.0507	0.1224	0.00138	0.00265
S1	~2120	23	52	98	40	1.43	0.349	0.0427	0.1001	0.00190	0.00282
S2	~2130	51	77	112	77	0.79	0.030	0.0057	0.0092	0.00326	0.00596
Refractory dust											
RD1	~3010	18	57	108	42	1.57	0.324	0.0631	0.1428	0.00139	0.00179
RD2	~2750	44	72	109	67	0.91	0.080	0.0063	0.0023	0.00360	0.00561

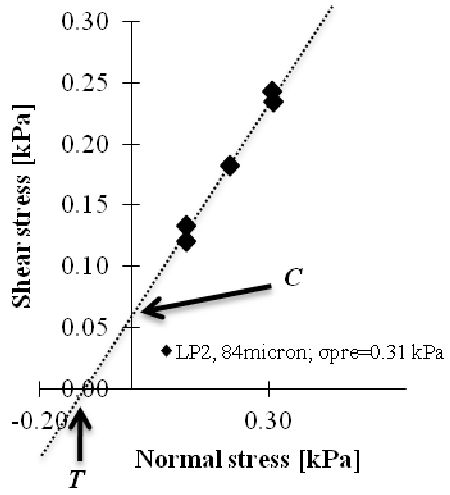

Figure 2 Plot of shear stress vs. normal stress at σ_{pre}=0.31 kPa, for lactose LP2

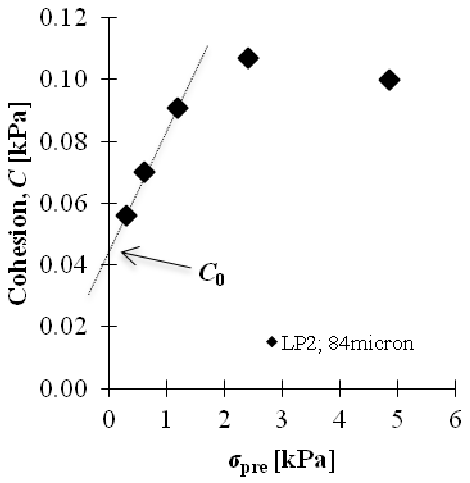

Figure 3 Plot of cohesion vs. pre-consolidation stress, σ_{pre}, for lactose LP2

RESULTS

The values estimated for C_0 and T_0 are listed in Table 1. The plot in Figure 4, C_0 versus d^*_{32}, is presented to show that there is some degree of correlation between these variables, as surmised in the introduction above, though the data appear to fall into two groupings; the milled lactose has a weaker dependence on d^*_{32} than the other materials.

Figure 5 shows C_0 plotted against T_0. It is apparent that there is a strong relationship between the two which can be expected to follow similar trends as they are both effectively bulk measures of inter-particle adhesive forces; henceforward we will confine our focus to C_0.

Figure 6 shows bed collapse profiles, typical of Geldart Group A powders (9), for lactose LP2 and LT1. The collapse profiles for sand S1 and S3 are similar to that of LT1; the other test materials have collapse profiles similar to LP2, except for lactose LP3 which is a Geldart Group B powder exhibiting rapid de-aeration.

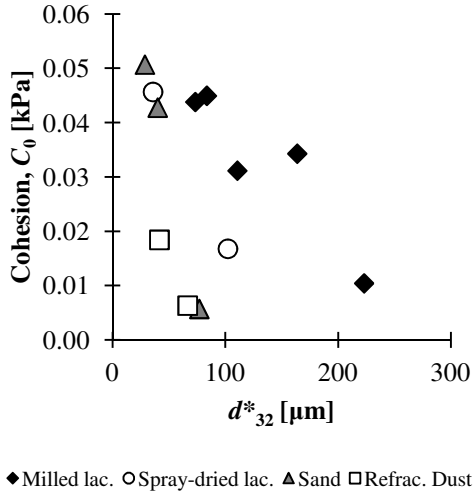

Figure 4 Plot of C_0 versus d^*_{32}

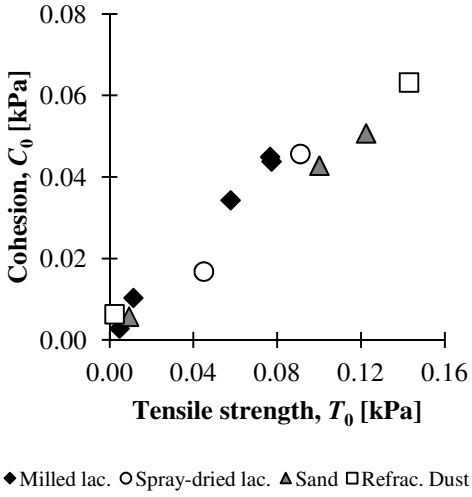

Figure 5 Plot of C_0 versus T_0

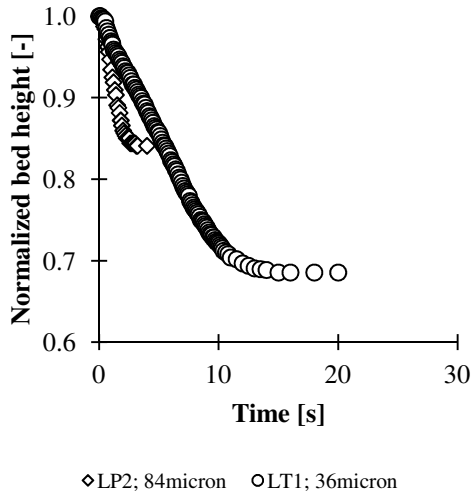

Figure 6 Bed collapse profiles of lactose LP2 and LT1

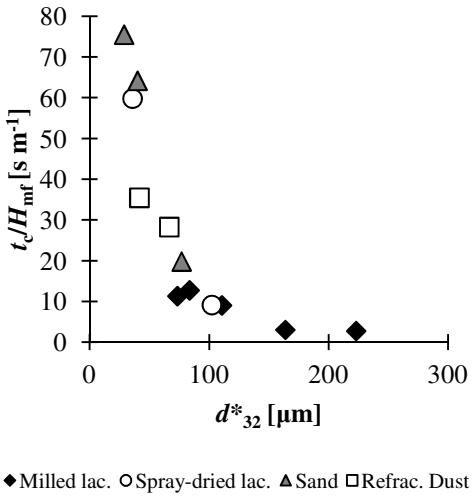

Figure 7 Plot of t_c/H_{mf} versus d^*_{32}

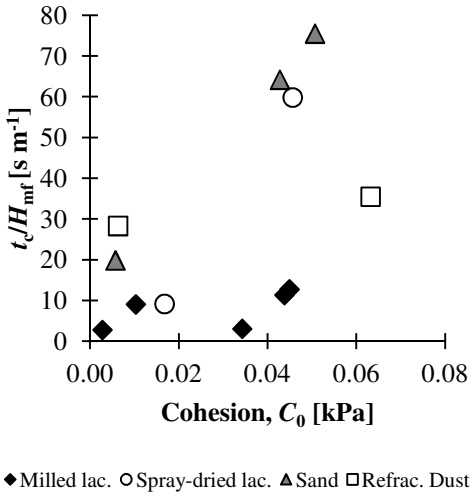

Figure 8 Plot of t_c/H_{mf} versus C_0

Figure 7 plots t_c/H_{mf} and d^*_{32}; t_c/H_{mf} decreases rapidly showing apparent inverse proportionality with d^*_{32}. In Figure 8, t_c/H_{mf} is plotted against C_0; consistent with Figure 4, the data fall into two groupings, one comprising the milled lactose, and the other comprising the other test materials.

DISCUSSION

The functional relationships between t_c/H_{mf} and material properties in the correlation due to Geldart and Wong (6), the findings of Khoe *et al.* (1), and the dependance of cohesion on $[\rho_B/(\rho_p\, d_{32})]$ noted by Saw *et al.* (5) where the ratio ρ_B/ρ_p implies a voidage term, together suggest $[t_c/H_{mf}]$ is proportional to $\{C_0[f(\text{distribution and fines content}), f(\varepsilon), f(\rho_p)]\}$. However, following preliminary empirical inspection of our data, it is apparent that further analysis is required to explain the observed trends, particularly, with regard to the characteristics of the size distributions.

CONCLUSIONS

Powder cohesion and tensile strength for zero applied stress have been estimated for lactose powders, sand and refractory dust, from measurements taken with an annular shear cell. The same powders have been used in bed collapse experiments and standardized collapse time measured for each. Standardized collapse time seems to correlate with powder cohesion, but the data for lactose and those for the mineral powders, sand and refractory dust, follow different trends.

ACKNOWLEDGEMENT

HYS acknowledges a PhD scholarship from the Riddet Institute and assistance from technical staff in the School of Engineering and Advanced Technology.

NOTATION

C	Powder cohesion [kPa]
C_0	Powder cohesion at zero pre-consolidation stress [kPa]
d_{10}	Particle diameter at which 10% of the sample is below a given size of a volume-weighted size distribution [μm]
d_{50}	Particle diameter at which 50% of the sample is below a given size of a volume-weighted size distribution [μm]
d_{90}	Particle diameter at which 90% of the sample is below a given size of a volume-weighted size distribution [μm]
d_{32}	Surface-volume mean diameter [μm]
d^*_{32}	Surface-volume diameter calculated from Mastersizer distribution data using bins equivalent to a full sieve analysis according to BS410 [μm]
F_{45}	Fines (<45 μm) fraction [-]
H_{mf}	Bed height at minimum fluidizing velocity [m]
n	Regression constant [-]
T	Powder tensile strength [kPa]
T_0	Powder tensile strength at zero pre-consolidation stress [kPa]
t_c	Time required for linear bed collapse, hindered settling [s]
$U_{mb,v}$	Minimum bubbling velocity determined by visual observation [m s^{-1}]
U_{mf}	Minimum fluidizing velocity [m s^{-1}]
ε	Voidage [-]
ε_{mb}	Bed voidage at minimum bubbling fluidization [-]
ε_{mf}	Bed voidage at minimum fluidization [-]
ρ_B	Bulk density of powder [kg m^{-3}]
ρ_g	Gas density [kg m^{-3}]
ρ_p	Particle density [kg m^{-3}]
σ_{pre}	Pre-consolidation stress [kPa]

REFERENCES

1. G.K. Khoe, T.L. Ip and J.R. Grace. Rheological and fluidization behaviour of powders of different particle size distribution. Powder Technol., 66: 127-141, 1991.
2. O. Molerus. Theory of yield of cohesive powders. Powder Technol., 12: 259-275, 1975.
3. O. Molerus. Effect of interparticle cohesive forces on the flow behaviour of powders. Powder Technol., 20: 161-175, 1978.
4. G. Bruni, P. Lettieri, D. Newton and D. Barletta. An investigation of the effect of the interparticle forces on the fluidization behaviour of fine powders linked with rheological studies. Chem. Eng. Sci., 62: 387-396, 2007.

5. H.Y. Saw, C.E. Davies, J.R. Jones, G. Brisson and A.H.J. Paterson. Particle cohesion of lactose powders at low consolidation stresses. Adv. Powder Technol., in revision.
6. D. Geldart and A.C.Y. Wong. Fluidization of powders showing degrees of cohesiveness – II. Experiments on rates of de-aeration. Chem. Eng. Sci., 40(4):653-661, 1985.
7. GEA Niro. Particle density, occluded air and interstitial air by air pycnometer. Available at http://www.niro.com/niro/cmsdoc.nsf/WebDoc/webb7ceec8 (accessed on October 3rd, 2012)
8. H.Y. Saw, C.E. Davies and A.H.J. Paterson. Tracking the transitions in gas-fluidized beds with measurements of pressure fluctuations. Proc. 5th Asian Part. Tech. Symp. 2012, Singapore, 2-5 July 2012, doi: 10.3850/978-981-07-2518-1_281.
9. D. Geldart. Types of gas fluidization. Powder Technol., 7(5): 285-292, 1973.